The International Young Researchers' Conference
DOI:

Synthesis and characterization of Fe doped TiO2 photocatalyst for the treatment of organic dye in wastewater

Hoang Son Thai
High School for Gifted Students, Hanoi National University of Education, Vietnam
thaihoangson08@gmail.com

Abstract

Photocatalysis is one of the effective methods to treat wastewater and degrade pollutants. Titania (TiO_2) is usually chosen based on its superior properties and its high performance as reported in many publications. By doping Fe, TiO_2 can gain some more advantages and become more effective in the visible light. In this work, TiO_2 and Fe doped TiO_2 samples are synthesized by precipitation method, and then are characterized by XRD, SEM-EDS, solid UV-Vis, physical adsorption techniques before photocatalytic tests for treating methyl orange in water. The samples possess fine particles sizes, high surface areas and are able to absorb light in UV region as expected but the photocatalytic activity in UV light of Fe doped TiO_2 is less than TiO_2 due to the decreased amount of TiO_2. Meanwhile, Fe doped TiO_2 catalyst exhibited a little higher activity in the visible light due to the little ability to absorb visible light and a reduced band gap energy.

Keywords: Photocatalysis; nano titania, Fe doped titania, precipitation

Introduction

Water pollution have always been a major concern of many countries, especially developing countries like Vietnam. Due to the lack of resources, inadequate infrastructure, and role of benefit in production, water sources have been polluted by some heavy metal and toxic organic substances [1-3]. Especially, in the traditional villages like Van Phuc, where different types of silk are produced, toxic organic dyes pollute significantly the water environment. Therefore, finding methods to solve the problem of water pollution is an interest of worldwide scientists, societies and governments.

The traditional processing methods of polluted water are mainly based on physico-chemical and biological treatment techniques. The adsorption method is one of the most used techniques among them to treat chemical contaminants in water because of its simple operation and the wide applicability of many adsorbents. Another effective solution is biological treatment because the high amount of the organic substances can be eliminated, but this method is less effective for chemicals that are difficult to be decomposed such as organic dyes... However, these methods have some limitations in practice, such as: complex operation, high

material and operating costs, generating by-products, requiring post- treatment or low efficiency [4, 5].

The photocatalytic semiconductor process is one of the advanced oxidation processes in which the semiconductors absorbing photon energy from light radiation to form hydroxyl radical (* OH). The photocatalytic process has been considered as an important process in the field of wastewater treatment in recent years. This process has many advantages such as the decomposition of organic matters can reach a completed level of inorganic, no post treatment is required, low investment and operation costs, performed under normal temperature and pressure conditions, using UV source or sunlight. TiO_2 and is one of the most interesting materials among semiconductors used as photocatalysts for many scientists and researchers [6-8].

Fe doped TiO_2 catalysts have been reported to be able to allow the photocatalytic activity occurred in the visible light region, which is more convenient for the practical application than undoped TiO_2 catalyst. The Fe-doped samples were found to be paramagnetic at room temperature (by magnetization measurements), with Fe acting as substitutional impurity at Ti sites in the anatase TiO_2 phase [9]. The catalytic activities of these materials are influenced significantly by the interaction between iron and titania phases. Synthesis methodology such as solgel, precipitation, hydrothermal also influences on the phase composition, crystal structure and therefore catalytic activity of the Fe doped TiO_2 catalysts. Nevertheless, good results have been reported for the visible light photocatalytic treatment of organic compounds in water by Fe doped TiO_2 [10-16].

In this work, TiO_2 and Fe doped TiO_2 was synthesized by gel-precipitation method. The catalytic activities of TiO_2 and 3 wt% Fe doped TiO_2 (corresponds to $Ti_{0.97}Fe_{0.03}O_2$ formulation) in the full range light, visible light and sun light were compared to show how appearance of Fe affects the photocatalysis efficiency to treat methyl orange (MO) in water. These catalysts have been examined for the treatment of methylene blue in visible light [9] but the comparison between full range light and visible light to clarify the role of Fe has never been done previously. Moreover, a practical test under true sun light is interesting to confirm the real application of the catalysts.

Experimental

Synthesis of Catalysts

TiO_2 and Fe doped TiO_2 samples are synthesized by gel-precipitation method. Figure 1a shows how TiO_2 sample was synthesized. First, 25ml of ethanol (99.7%, Merck) was magnetic stirred with 450ml distilled water to form solution 1. Then, 2.5ml Titanium isopropoxide TTIP (97%,

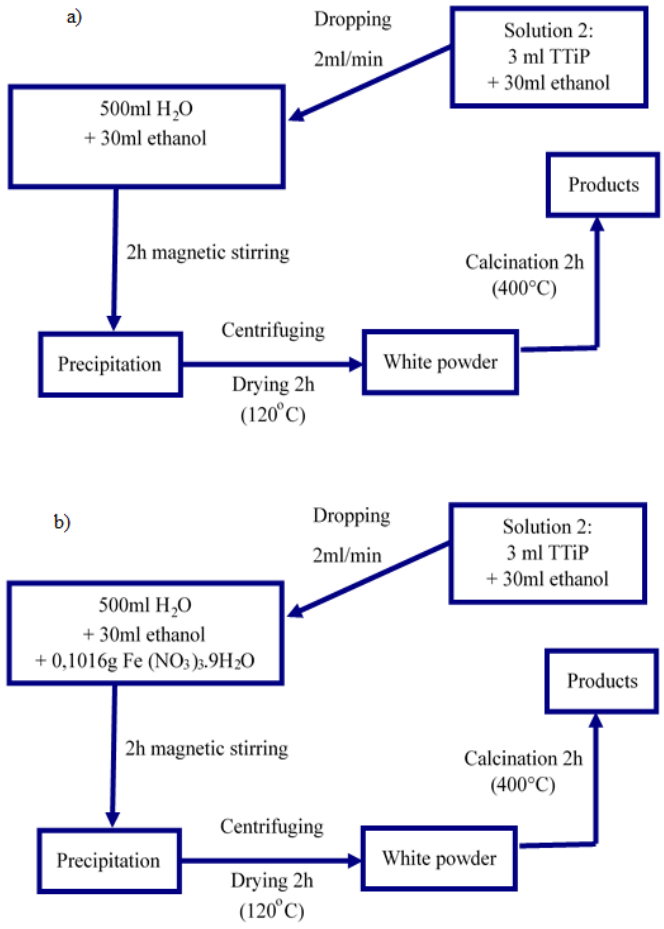

FIGURE 1. Synthesis procedure for (a) TiO_2 and (b) 3 wt% Fe doped TiO_2

Aldrich) is mixed with 25ml of ethanol by magnetic stirring to form solution 2. Next stage, solution 2 was slowly dropped (2ml/min) into solution 1 while solution 1 was kept stirring. When solution 2 was fully dropped, the obtained solution was kept stirring for two hours. After stirring process had finished, the solution became a white gel. The white gel then was centrifuged (2000 round/min), for 2 mins and then dried in vacuum for 2 hours at 120°C. Finally, the sample was ground and calcined at 400°C for 2 hours. Then, TiO_2 sample had been successfully created. To synthesize the 3 wt% Fe doped TiO_2 sample, the above experiment was repeated with putting 0,1016g Fe $(NO_3)_3.9H_2O$ (Merck) in solution 1 before starting the stirring process (Figure 1b).

Characterization of Catalysts

The crystalline phase of the samples was investigated by X-ray power Diffraction using a Bruker D8 Ax XRD-diffractometer (Germany). XRD patterns were obtained with Cu-Kα irradiation (40kV, 40 mA) at the 2θ ranging from 20 to 80°. The morphology of the samples was observed by a Field Emission Scanning Electron Microscope (a JEOL JSM-7600F, USA), the elements composition was determined by a dispersive energy X-ray spectrometer EDS (Oxford Instruments 50 mm^2 X-Max, England). The specific surface area, pore volume and pore diameter were measured via N_2 adsorption/desorption isotherms using the Brunauer-Emmett-Teller (BET) method on a Micromeritics Gemini VII 2390 analyzer. The solid UV-Vis spectra of the catalysts were obtained using an Avantes UV-VIS spectrometer.

Photocatalytic Test

The photodegradation of MO was performed in a batch scale reactor. A xenon lamp 300W 15A LOT Quantum Design with full range light of wavelength from 200 to 2500 nm was placed in front of a quartz tube containing 30 ml MO solution 10 ppm and 50 mg catalyst, which was fitted with a water cooling jacket to maintain a steady temperature of 25 °C. The light is placed at the center of the reactor and solution contents were kept uniformly distributed by using a magnetic stirrer. In the case of performing the reaction in the visible light region, an UV filter was placed in the lamp. After keeping in dark for 30 min in each run to reach adsorption-desorption equilibrium state, an aliquot of solution was sampled by a pipet and filtered through a 0.22 μm syringe filter. The MO concentration was determined by an Avantes UV-VIS spectrometer.

The MO degradation by the photocatalysts was determined by calculating the conversion of MO as follow:

$$C = \frac{Ct}{Co - Ct} \quad (1)$$

Where C_o is the initial concentration of MO solution and C_t is the concentration of MO solution in time, and t is reaction time (min).

Results and Discussion

Characterization of the Catalysts

Surface areas, average pore sizes and pore volumes of the synthesized samples are shown in Table 1, indicating that the samples possess high surface areas. Especially, the addition of Fe increased significantly surface area of the sample, which may represent a change of structure. This high surface area has never been reached for the same type of sample [9], showing that the characteristics of the materials depend significantly on the specific synthesis, even the speed of droplet adding or the rate of heating rate during calcination. Accordingly, TiO_2 sample possess much higher average pore width than Fe doped TiO_2 sample. Both samples are mesoporous as indicated in the adsorption – desorption isotherm in Fig. 2 (a). The pore distribution curves of two samples in Fig. 2 (b) indicated that Fe doped TiO_2 sample possesses much higher ratio of mesopore (from 20 to 40 Å) to macropores (from 250 to 600 Å) than that of TiO_2 sample, which fits well with the higher surface area of the Fe doped TiO_2 sample.

TABLE 1. Surface areas, average pore sizes and pore volumes of the synthesized samples

	TiO_2	Fe doped TiO_2
BET Surface Area (m^2/g)	89.32	237.69
BJH Adsorption average pore width (Å)	186.13	69.29
BJH average pore volume (cm^3/g)	0.47	0.38

XRD analysis of the samples shows that they all exhibited anatase structure, the presence of Fe in the sample could not be detected due to a low amount of the doped element.

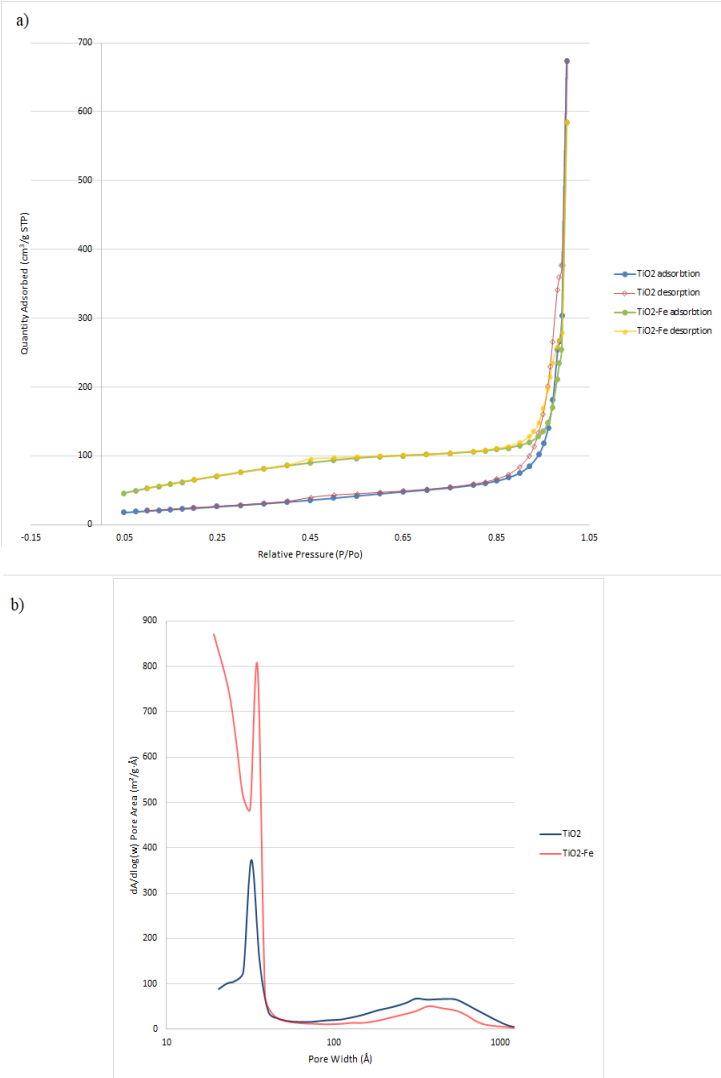

FIGURE 2. (a) N_2 adsorption – desorption isotherm of the synthesized samples and (b) Pore distribution of the synthesized samples

SEM images of the synthesized samples in Figure 3 show that TiO_2 as depicted in Figure 3 (a) exhibited extremely fine particles, just around 15 nm. Meanwhile, Fe doped TiO_2 in Figure 3 (b) resulted in particles with approximate same size, and these particles have unspecify shapes. This means, the addition of Fe doesn't influence on sizes of TiO_2 particles.

a)

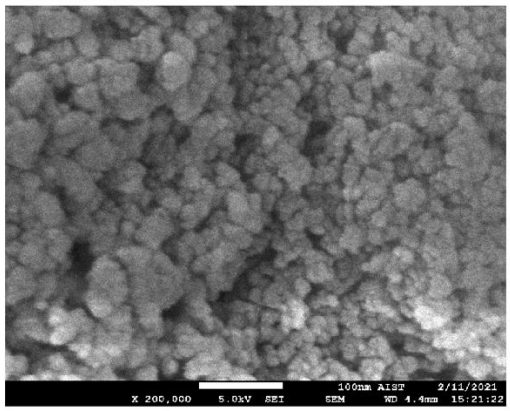

b)

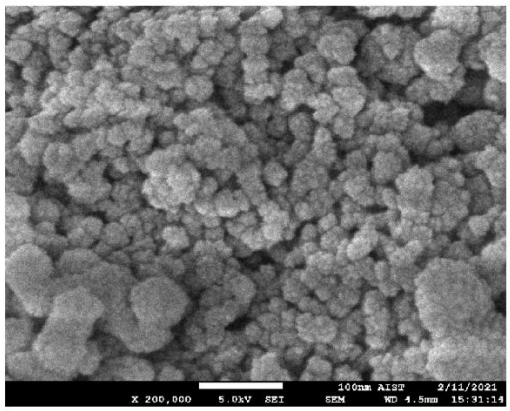

FIGURE 3. SEM images at magnification of 200.000 times of TiO_2 (a) and Fe doped TiO_2 (b)

EDS mapping taken in Fe doped TiO_2 sample in Fig. 4 shows fine distribution of main element as Ti and O while the presence of Fe is much fewer due to its low quantity (3 wt%). Fig. 5 present the map of EDS measurements corresponding to the result in Table 2. The results prove the presence of Fe in the sample with approximately the same ratio as calculated from theoretical composition (3 wt%). Thus, the addition of Fe to TiO_2 is successful.

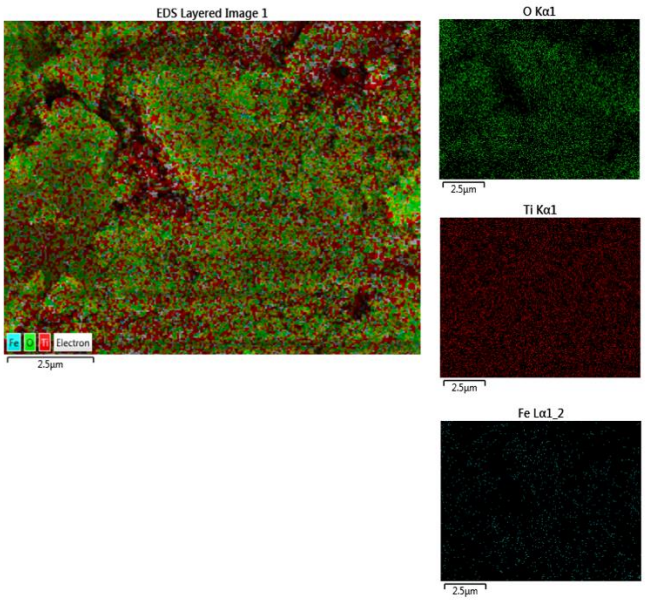

FIGURE 4. EDS mapping of Fe doped TiO_2 sample: a) all element mapping, b) O mapping, c) Ti mapping, d) Fe mapping

TABLE 2. Ratio of element in Fe doped TiO_2 sample measured by EDS

Position	Ratio of Ti (Wt%)	Ratio of O (Wt%)	Ratio of Fe (Wt%)
Spectrum 2	63.8	35.8	0.4
Spectrum 3	59.9	36.7	3.4
Spectrum 4	51.5	45.2	3.3
Spectrum 6	61.5	38.4	0.1
Spectrum 12	50.1	47.2	2.7

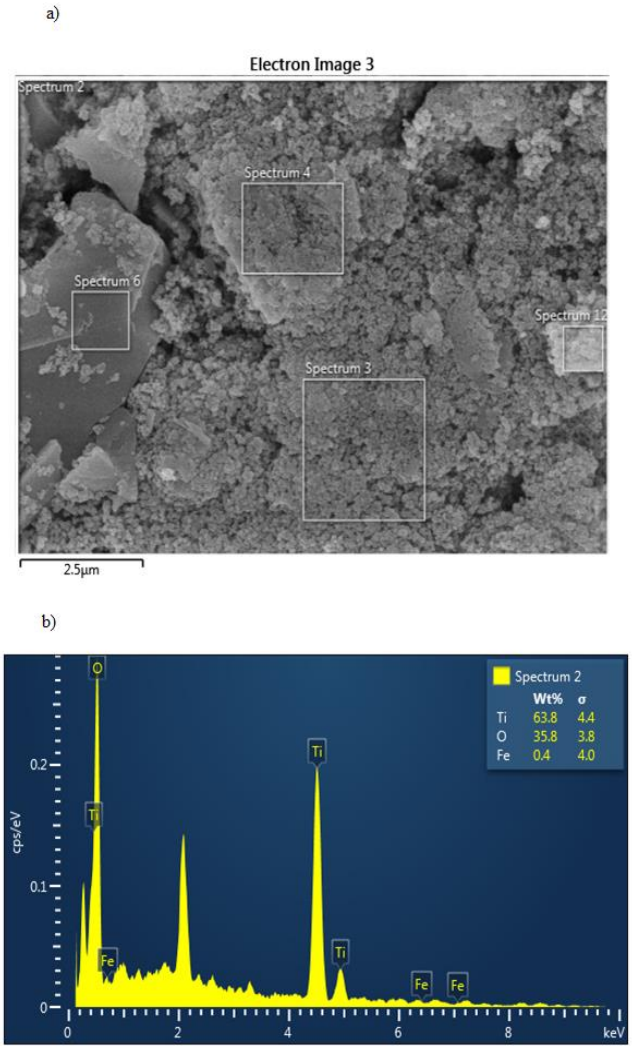

FIGURE 5. The map of EDS measurements: a) the map of different points taken the EDS, b) EDS spectrum of point 2

The solid UV-Vis result (Figure 6 (a)) show that TiO_2 sample can absorb the lights in the wavelength region from 200 to 400 nm, peaked at about 300 nm. That means that TiO_2 catalyst can only absorb light in the UV region (from 100 to 400 nm). Meanwhile, Fe doped TiO_2 can absorb wider wavelength lights from 200 nm to 700 nm. However, the ability to absorb lights at visible region (from 380 – 760 nm) of this catalyst is only a little. Thus, the 3 wt% Fe doped sample not yet absorbed intensively the visible light as expected. That may be due to 3wt% (0.03 mol of Fe replaced for Ti in $Ti_{1-x}Fe_xO_2$ structure) is not a suitable ratio for iron ions (previous study showed that the highest activity was obtained when 0.06 mol of Fe replaced for Ti [9]), therefore the ability to absorb visible lights was not improved.

The solid UV-vis result also depict that due to the maximum absorbed wavelength increased, the band gap energy may decrease. This was proven by calculating the band gap energy as seen in Fig. 6 (b), which are 3.15 and 2.8 eV for TiO_2 and Fe doped TiO_2 sample, respectively.

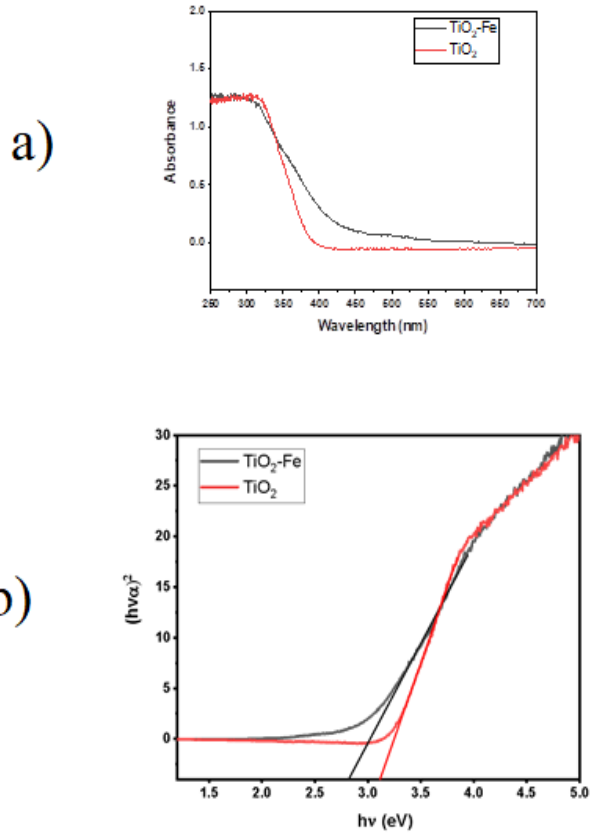

FIGURE 6. (a) Solid UV-Vis Spectra of the synthesized samples, (b) Graph calculating band gap energy of the synthesized samples

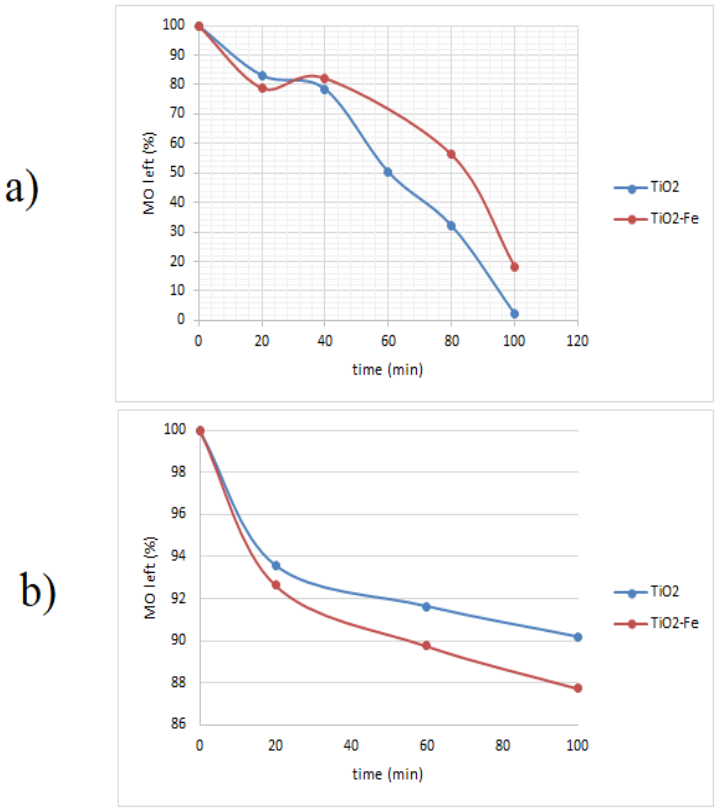

FIGURE 7. (a) Photocatalytic activity under full range light of TiO_2 and Fe doped TiO_2 samples, (b) Photocatalytic activity under visible light of TiO_2 and Fe doped TiO_2 samples

Photocatalytic Activity

The graph expressed the degradation of MO under full range light (Figure 7 (a)) shows how the photocatalysis to treat MO. TiO_2 can almost treat MO fully in 100 minutes and has a steadily decreasing trend. Meanwhile, the curve for Fe doped TiO_2 fluctuates inconstantly and only declined the proportion of MO by 80% in 100 minutes. Thus, in our case, the addition of Fe has a negative influence on the MO treating trend. This may be due to the presence of Fe, if not doped correctly in the TiO_2 structure, results in free Fe oxides outside of TiO_2 structure, which contributes to lower the concentration of TiO_2 in the sample and thus, decreases active sites and the activity.

The full range light is a simulation of the sun light. Therefore, the samples were also tested under the sun light to observe the phenomena.

Under the rare stirring condition, it can be seen that the TiO_2 sample can de-color the MO solution in a shorter time (38 hours) than that of Fe doped TiO_2 sample (de-color after 48 hours under sun light). The phenomenon was photographed as seen in Figure 8.

To explain the reason of the degradation of MO due to UV light or visible light, the samples were also tested under visible light when applied a UV filter in the Xe lamp. The results presented in Figure 7 (b) shows that the samples exhibited much smaller activity under the visible light, only about 20% MO was degraded after 100 minutes of the illumination. Oppositely to the case of illumination under full range light, Fe doped TiO_2 sample exhibited a slightly higher activity than the undoped TiO_2 sample. This is in a good agreement with what observed in solid UV-vis measurement of these samples, which showing that Fe doped TiO_2 sample may absorb more light

in the visible region. Thus, the ability to degrade MO of TiO_2 and Fe doped TiO_2 sample under the full range light as presented in Fig.7 (a) is mainly due to the activity of TiO_2 under UV light. Fe doped TiO_2 composition contributed more to the activity under the visible light region but the activity was still low. However, it is a good indication to confirm the photocatalytic activity of the Fe doped TiO_2 catalysts in the visible light. If an optimal ratio of Fe doping can be applied, the photocatalytic activity in the visible light may be much improved.

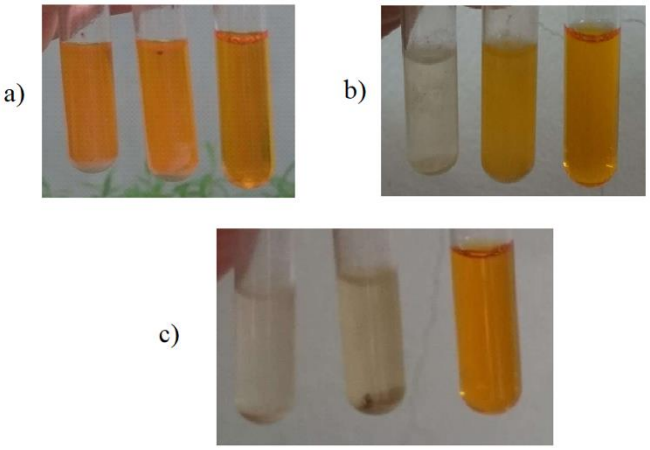

FIGURE 8. De-coloration of the MO solution under the sun light: a) before the illumination of sun light, b) after the illumination of sun light for 38 hours, c) after the illumination of sun light for 48 hours, left - TiO_2 sample, middle - Fe doped TiO_2 sample, right – blank sample (no catalyst)

Conclusion

By doping Fe to TiO_2 nano particles, changes appeared on its characterization and photocatalytic activity. Although not all the changes are advantages, this study shows that the Fe doped TiO_2 may work in full range light region and sun light. The addition of Fe to TiO_2 results in no remarkable change on particle size and crystal structure. Despite of the decrease in photocatalytic activity in the full range light region, the addition of Fe showed the evidence of the slight change in the ability to absorb light from UV region to visible region.

The results also show that the Fe doped TiO_2 can treat several types of color organic dyes as methylene blue in the previous work [9] and methyl orange in this work, thus, it may apply to treat wastewater from the traditional villages in Vietnam like Van Phuc. Further investigation on changing the ratio of Fe in the Fe doped TiO_2 catalyst might help the Fe doped TiO_2 catalyst to treat the wastewater more effectively in visible light region.

Acknowledgments

The authors acknowledge Dr. Nguyen Duc Dung – Advanced institute of science and technology, Hanoi university of Science and Technology for SEM-EDS measurement.

References

[1] Liu, Y., Zhou, S., Yang, F., Qin H, Kong Y (2016). Degradation of phenol in industrial wastewater over the F–Fe/TiO2 photocatalysts under visible light illumination. *Chinese Journal of Chemical Engineering*, *24*(12), 1712-1718. https://doi.org/10.1016/j.cjche.2016.05.024

[2] The, C., Mohamed, A. (2011). Roles of titanium dioxide and ion-doped titanium dioxide on photocatalytic degradation of organic pollutants (phenolic compounds and dyes) in aqueous solutions: A review. *Journal of Alloys and Compounds*, *509*(5), 1648-1660. https://doi.org/10.1016/j.jallcom.2010.10.181

[3] Eldred, R. N. (2001). *Chemistry for the Graphic Arts* (3rd ed.). Pennsylvania, USA: Graphic Arts Technical Foundation.

[4] Sangeetha, R., Basha, C. (2007). Chemical or electrochemical techniques, followed by ion exchange, for recycle of textile dye wastewater. *Journal of Hazardous Materials, 149*(2), 324-330. https://doi.org/10.1016/j.jhazmat.2007.03.087

[5] Rice, E. W., Baird B. R., Eaton A. D., Clescerei L. S. (2012). *Standard Method for the Examination of Water and Wastewater* (22nd ed.). Washington D.C., USA: American Public Health Association.

[6] Nguyen, T.H., Vu, A.T., Dang, V.H., Wu, J.C.S., Le, M.T. (2020). Photocatalytic Degradation of Phenol and Methyl Orange with Titania-Based Photocatalysts Synthesized by Various Methods in Comparison with ZnO–Graphene Oxide Composite, *Topics in Catalysis, 63*, 1215–1226. https://doi.org/10.1007/s11244-020-01361-5

[7] Carp, O., Huisman, C. L., Reller, A. (2004). Photoinduced reactivity of titanium dioxide. *Progress in Solid State Chemistry*, *32*(1–2), 33-177. https://doi.org/10.1016/j.progsolidstchem.2004.08.001

[8] Chen, J., Qiu, F., Xu, W., Cao, S., Zhu, H. (2015). Recent Progress in Enhancing Photocatalytic Efficiency of TiO2-based Materials. *Applied Catalysis A: General*, *495*, 131-140. https://doi.org/10.1016/j.apcata.2015.02.013

[9] Dang, X.T., Vu, Q.T., Nguyen, M.N., Nguyen, C.K., Tran, D.L. (2016). Effects of Fe Doping on the Structural, Optical, and Magnetic Properties of TiO2 Nanoparticles, *Journal*

of Electronic Materials, 45, 6033–6037. https://doi.org/10.1007/s11664-016-4825-6

[10] Luo, H., Yua, S., He, F., Li, L., Zhong, M., Dong, N., Su, B. (2021). An important phenomenon in Fe2O3-TiO2 photocatalyst: Ion-inter-doping, *Solid State Sciences*, *113*, 106538. https://doi.org/10.1016/j.solidstatesciences.2021.106538

[11] Khasawneh, O. F. S., Palaniandy, P. (2021) Removal of organic pollutants from water by Fe2O3/TiO2 based photocatalytic degradation: A review, *Environmental Technology & Innovation*, *21*, 101230. https://doi.org/10.1016/j.eti.2020.101230

[12] Nguyen, C.K., Nguyen, V.K., Nguyen, H.A., Do, T.N., Nguyen, V.M. (2011). The origin of visible light photocatalytic activity of N-doped and weak ferromagnetism of Fe-doped TiO2 anatase, *Advances in Natural Sciences: Nanoscience and Nanotechnology*, *2*, 015008. https://doi.org/10.1088/2043-6262/2/1/015008

[13] Larumbe, S., Monge, M., Gómez-Polo, C. (2015). Comparative study of (N, Fe) doped TiO2 photocatalysts, *Applied Surface Science, 327*, 490-497. https://doi.org/10.1016/j.apsusc.2014.11.137

[14] Li, Z., Shen, W., He, W., Zu, X. (2008). Effect of Fe-doped TiO2 nanoparticle derived from modified hydrothermal process on the photocatalytic degradation performance on methylene blue, *Journal of Hazardous Materials, 155*(3), 590-594. https://doi.org/10.1016/j.jhazmat.2007.11.095

[15] Sood, S., Umar, A., Mehta, S.K., Kansal, S.K. (2015). Highly effective Fe-doped TiO2 nanoparticles photocatalysts for visible-light driven photocatalytic degradation of toxic organic compounds, *Journal of Colloid and Interface Science, 450*, 213-223. https://doi.org/10.1016/j.jcis.2015.03.018

[16] Ali, T., Tripathi, P., Azam, A., Raza, W., Ahmed, A.S., Ahmed, A., Muneer, M. (2017). Photocatalytic performance of Fe-doped TiO2 nanoparticles under visible-light irradiation, *Materials Research Express, 4*(1), 015022. https://doi.org/10.1088/2053-1591/aa576d